Journal of Neuro-Oncology (2019) 142:103–109
https://doi.org/10.1007/s11060-018-03068-w

CLINICAL STUDY

Heterogeneity of glioblastoma with gliomatosis cerebri growth pattern on diffusion and perfusion MRI

Alex Förster[1] · Stefanie Brehmer[2] · Marcel Seiz-Rosenhagen[2] · Iris Mildenberger[3] · Frank A. Giordano[4] · Holger Wenz[1] · David Reuss[5,6] · Daniel Hänggi[2] · Christoph Groden[1]

Received: 15 September 2018 / Accepted: 30 November 2018 / Published online: 18 December 2018

Abstract

Background and purpose Gliomatosis cerebri (GC) is a rare growth pattern of glioblastoma whose diffuse nature is reflected by unspecific, relatively uniform findings on conventional MRI. In the present study we sought to evaluate the additional value of diffusion (DWI) and perfusion weighted (PWI) MRI for a more detailed characterization.

Methods We analyzed the MRI findings in patients with histologically proven glioblastoma with GC growth pattern with a specific emphasis on T2 lesion pattern, volume, relative apparent diffusion coefficient (rACD), and relative cerebral blood volume (rCBV) and compared these to age-/gender-matched patients with localized glioblastoma.

Results Overall, 16 patients (median age 59.5 years, 4 male) were included in the study. Of these, 8 patients had a glioblastoma with GC growth pattern, and 8 a classical localized growth pattern. While the median rADC (1.27 [IQR 1.12–1.41]) within the T2 lesion was significant lower in glioblastoma with GC growth pattern compared to localized glioblastoma (1.74 [IQR 1.45–1.96]; p = 0.003), the median T2 lesion volume and rCBV within the T2 lesion did not differ significantly. Furthermore, six patients with glioblastoma with GC growth pattern showed focal areas with significantly reduced rADC (p = 0.043), and/or increased rCBV (p = 0.028).

Conclusions Lower rADC in glioblastoma with GC growth pattern might reflect the diffuse tumor cell infiltration whereas focal areas with decreased rADC and/or increased rCBV probably indicate high tumor cell density and/or abnormal tumor vessels which may be useful for biopsy guidance.

Keywords Glioblastoma · Gliomatosis cerebri · Heterogeneity · Diffusion-weighted imaging · DWI · Perfusion-weighted imaging · PWI

Introduction

Glioblastoma is the most common primary brain tumor with short progression free survival of approximately seven and an overall survival of approximately 15 months [1, 2]. The tumor grows highly invasive and its cells are able to migrate along pre-existing structures such as blood vessels and white matter tracts [3, 4]. Glioblastoma occurs in different growth patterns such as localized, multifocal, and multicentric [5]. The latter two growth patterns describe glioblastoma with multiple enhancing lesions either embedded within a larger region of signal alterations on T2-weighted images as is the case with multifocal glioblastoma, or distinct without connecting signal alterations on T2-weighted images as is the case with multicentric glioblastoma. Another growth pattern is the so-called gliomatosis cerebri (GC) which has been regarded as a distinct tumor entity for a long time [6]. The diffuse nature of GC growth pattern is reflected by unspecific findings on conventional MRI with wide-spread signal alterations on T1- and T2-weighted images involving at least three cerebral lobes and a lack of or minimal contrast enhancement [7]. In some studies a further categorization is used based on the presence of a focal mass [8]. As complete resection is not possible in glioblastoma with GC growth pattern, a minimal invasive biopsy is usually performed to establish the diagnosis. However, histopathological analysis can be inconclusive, and repeated biopsy may be necessary.

Alex Förster and Stefanie Brehmer contributed equally to the manuscript.

✉ Alex Förster
Alex.Foerster@umm.de

Extended author information available on the last page of the article

Recently, it has been suggested that regional differences of glioblastoma aggressiveness correlate to specific patterns in diffusion-weighted (DWI) and perfusion weighted MRI (PWI). In more detail, a reduced relative apparent diffusion coefficient (rADC) and increased relative cerebral blood volume (rCBV) have been shown to be indicative for a more aggressive (local) phenotype [9, 10]. Generally, data on imaging features of GC is scarce, and usually no distinction is made between glioblastoma and other gliomas [11–15].

Therefore we aimed to (1) describe lesion patterns on fluid attenuated inversion recovery (FLAIR) images, and to evaluate the additional value of (2) DWI as well as (3) PWI for a more detailed characterization of glioblastoma with GC growth pattern in the present study.

Materials and methods

Patients

In the GC group, all patients with glioblastoma with GC growth pattern identified from a prospectively collected MRI report database (2012–2018) were included. In the control group, patients with localized glioblastoma matched to the GC group according to age, sex, and IDH mutation were included. Patients in both groups were analyzed and compared with regard to MRI findings with special focus on T2 lesion pattern and volume, as well as relative apparent diffusion coefficient (rACD), and relative cerebral blood volume (rCBV) within the T2 lesion.

MRI studies

Magnetic resonance imaging was performed on a 1.5 T MR system (Magnetom Sonata or Avanto, Siemens Medical Systems, Erlangen, Germany) or a 3 T MR system (Magnetom Trio, Siemens Medical Systems). A standardized protocol was used in all patients including (1) transverse, coronal and sagittal localizing sequences followed by transverse oblique contiguous images aligned with the inferior borders of the corpus callosum (applied on sequences 2–6); (2) T1-weighted images; (3) T2-weighted images; (4) T2*-weighted gradient echo (GRE) images or susceptibility-weighted images; (5) diffusion-weighted images (DWI); (6) fluid attenuated inversion recovery (FLAIR) images; and (6) dynamic susceptibility contrast (DSC) perfusion-weighted images (PWI) following the first pass of contrast bolus through the brain. The contrast agent gadoteric acid (Dotarem, Guerbet, Aulnay-sous-Bois, France) was bolus injected by a power injector (Spectris MR injection system, Medrad, Volkach, Germany) with a dose of 0.1 mmol/kg of body weight at a rate of 4 ml/s. Afterwards (7) T1-weighted images identical to (2) were completed. Parameters of FLAIR, DWI, and PWI are given in Table 1.

Table 1 Sequence parameters of T1-weighted, FLAIR, and perfusion-weighted images at the department's MRI scanners

Sequence	Parameters	MRI scanner		
		1.5 T Siemens Sonata	1.5 T Siemens Avanto	3 T Siemens Trio
FLAIR	FOV	230×205	230×205	230×230
	Number of slices	24	24	24
	ST	5	5	5
	TR	8500	9000	9000
	TE	115	89	134
	TI	2400	2500	2500
DWI	FOV	230×230	230×230	230×230
	Number of slices	24	24	24
	ST	5	5	5
	TR	4400	4000	4000
	TE	101	96	91
PWI	FOV	230×230	230×230	230×230
	Number of slices	12	19	24
	ST	6	5	5
	TR	1500	1430	1770
	TE	46	30	32
	Flip angle	90	90	90

FOV field of view (mm×mm), *ST* slice thickness (mm), *TR* repetition time (ms), *TE* echo time (ms), *TI* inversion time (ms)

Postprocessing

The postprocessing of the PWI was performed by a commercial software package: Aycan Osirix Pro v2.04; Aycan Medical Systems, LLC, Rochester, NY, USA, and IB Neuro v1.1; Imaging Biometrics, LLC, Elm Grove, WI, USA. After transferring PWI to an off-line workstation and removing baseline points collected during the first 5 s, we generated whole-brain rCBV maps by using all default options including leakage correction: (1) automated detection of brain tissue mask for voxels used in CBV calculation, (2) automated detection of contrast arrival within brain mask voxels to define the pre-bolus baseline and integration intervals, and (3) leakage correction based on Boxerman et al. [16]. We normalized all rCBV maps to mean CBV from a 1 cm ROI within the contralateral frontoparietal normal-appearing white matter.

MRI analysis

All assessments were performed independently by two investigators (AF, HW), who then compared results and agreed mutually in cases with differing ratings. Anatomical lesion distribution was determined according to the maps by Tatu et al. and categorized in (1) frontal lobe, (2) temporal lobe, (3) insular lobe, (4) parietal lobe, (5) occipital lobe, (6) limbic lobe, (7) basal ganglia, (8) thalamus, (9) corpus callosum, (10) brainstem, and (11) cerebellum [17, 18]. Manual volumetric segmentation was performed on anonymized images by one of the investigators (AF) with the open source software MRIcron (http://www.mccauslandcenter.sc.edu/mricro/mricron/) [19]. Segmentation was performed on contrast-enhanced T1 weighted and FLAIR images according to the Vasari MR feature guide v.1.1 (https://wiki.nci.nih.gov/display/CIP/VASARI). In general, a region of interest was measured by defining a global threshold, and edited manually as necessary, after masking with a rough manual delineation of the lesion in order to exclude microangiopathic lesions, hemorrhage, macrovessels, cysts, or central necrosis. Since differentiation of vasogenic edema and non-enhancing tumor is difficult in glioblastoma we did not use separate definitions but defined hyperintense lesions comprising vasogenic edema and non-enhancing tumor on FLAIR images. Thus, three different tumor compartments were classified: enhancing tumor, necrosis, and hyperintense lesions comprising non-enhancing tumor and vasogenic edema. Contrast-enhanced tumor was defined on post-contrast T1 weighted images in comparison to pre-contrast T1-weighted images excluding hemorrhage. Necrosis was defined as a region within the tumor that showed absence of central enhancement and had a hyperintense signal on FLAIR images. Hyperintense lesions comprising non-enhancing tumor and vasogenic edema were classified on FLAIR images. As segmentations were made on the "exact match" FLAIR images naturally co-registered to the ADC and rCBV maps, no additional registration was performed. All ADC and rCBV maps completely covered the lesions in question. Median lesion rADC and rCVB were extracted from ADC and rCBV maps naturally co-registered to hyperintense lesion segmentations on FLAIR images. Focal areas of reduced diffusion and/or increased rCBV within the hyperintense lesion on FLAIR images were delineated manually on ADC and/or rCBV maps after thorough visual inspection.

Statistical analysis

All statistical analyses were performed using Statistical Product and Service Solutions (SPSS) statistics for Windows (Release 17.0; SPSS, Chicago, IL, USA). Descriptive data was analyzed by use of χ^2 based tests, or the Mann–Whitney U test as appropriate. Comparisons between rACD and rCBV were performed using a Mann–Whitney U test or the Wilcoxon test as appropriate. All statistics was performed with a 0.05 level of significance.

Results

Baseline characteristics, clinical presentation, and outcome

In the GC group, eight patients (median age 64.5 [IQR 50–77.5] years, two male) were included in the analysis. Clinical symptoms included seizures in four patients, dizziness in two patients, as well as headaches, personality changes, psychomotor slowing, lack of concentration, disorientation, facial palsy, and hemineglect in one patient respectively. In the control group, eight patients (median age 59.5 [IQR 50.25–71] years, two male) were included. Overall, six patients had a partial resection, and two patients a biopsy only. In two patients repeated biopsy was necessary as initial histopathological analysis was inconclusive. Follow-up was available in seven patients. At the end of the follow-up period, three patients were still alive. Median survival was 7.3 (95% CI 4.3–14.9) months; median progression-free survival 4.6 (95% CI 2.8–7.7) months.

MRI analysis

FLAIR images

In the GC group, all patients presented with widespread hyperintensities involving at least three cerebral lobes. In detail, involvement of the frontal lobe was observed in eight patients, the temporal lobe in eight patients, the insular lobe

in six patients, the parietal lobe in five patients, the limbic lobe in five patients, the basal ganglia in five patients, the thalamus in two patients, and the corpus callosum in three patients. No involvement of the occipital lobe, brainstem, or cerebellum was seen. The average volume of the correlating FLAIR hyperintensity was 72.1 ml (IQR 36.1–86.4). In the control group, all patients demonstrated hyperintensities of varying extent around the contrast enhancing lesion with a median volume of 53.4 ml (IQR 19.0–98.6). Volumes of FLAIR hyperintensities did not differ significantly between the GC group and the control group ($p = 0.57$).

Postcontrast T1-weighted images

In the GC group, none of the patients demonstrated contrast enhancement within the hyperintense lesions on FLAIR images. In the control group, all patients demonstrated contrast enhancing lesions of varying extent.

ADC maps

In the GC group, the median rADC within the hyperintense lesion on FLAIR images (1.27 [IQR 1.12–1.41]) was significantly lower than within the perifocal hyperintense lesion on FLAIR images in the control group (1.74 [IQR 1.45–1.96]; $p = 0.003$). Furthermore, five patients in the GC group showed focal areas with significantly reduced rADC (1.01 [IQR 0.87–1.17]; $p = 0.043$) in comparison to the entire hyperintense lesion (Fig. 1). In five patients this focal area was already observed on the first MRI, while in one patient it occurred in the clinical course (Fig. 2). In four of these patients, stereotactic/open biopsy or partial resection from this area was performed and pathohistological analysis revealed glioblastoma.

rCBV maps

In the GC group, the median rCBV within the hyperintense lesion on FLAIR images (1.74 [IQR 1.39–3.12]) did not differ significantly from that within the perifocal hyperintense lesion on FLAIR images in the control group (2.31 [IQR 1.75–2.87]; $p = 0.51$). In six patients in the GC group focal areas with significantly increased rCBV (2.66 [IQR 2.25–4.34]) compared to the entire hyperintense lesion ($p = 0.028$) were found. In five patients, these focal areas corresponded well to the observed lesions with reduced rADC. In another patient no corresponding focal area with reduced rADC was seen. In this patient, partial resection from this area was performed and pathohistological analysis revealed glioblastoma.

Discussion

GC is a rarely occuring growth pattern of glioblastoma whose diffuse nature is reflected by unspecific, relatively homogenous findings on conventional MRI. In the present study we sought to evaluate the additional value of DWI and PWI for a more detailed characterization of glioblastoma with GC growth pattern to allow a more robust separation to non-disseminated growth patterns. We found three novel and essential features: (1) glioblastoma with GC growth pattern showed a generally decreased rADC within the T2 lesion in comparison to localized glioblastoma, as well as focal areas with (2) significantly reduced rADC, and/or (3) increased rCBV.

On DWI, glioblastoma with GC growth pattern showed a generally decreased rADC possibly representing the diffusely infiltrating tumor cells. In newly diagnosed treatment-naive localized glioblastoma, the surrounding T2 lesion is regarded as a combination of tumor cell infiltration and vasogenic edema which usually cannot be distinguished based on MRI findings [20]. Thus, the higher rADC in the control group might be explained by a predominant vasogenic edema component in the T2 lesion. The observed focal areas with decreased rADC in glioblastoma with GC growth pattern most likely reflect the localized increased cellularity within the tumor. Interestingly, comparable

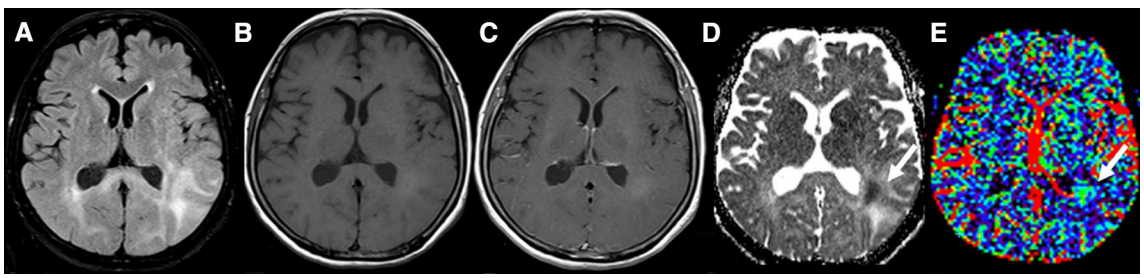

Fig. 1 MRI examination in an 81-year-old patient with glioblastoma with GC growth pattern. **a** FLAIR images demonstrate widespread hyperintensities in both hemispheres. **b** Comparison of native and **c** contrast-enhanced T1-weighted images demonstrates no contrast enhancement. **d** ADC maps show a focal area of reduced ADC (arrow). **e** rCBV maps show a focal area of increased rCBV (arrow)

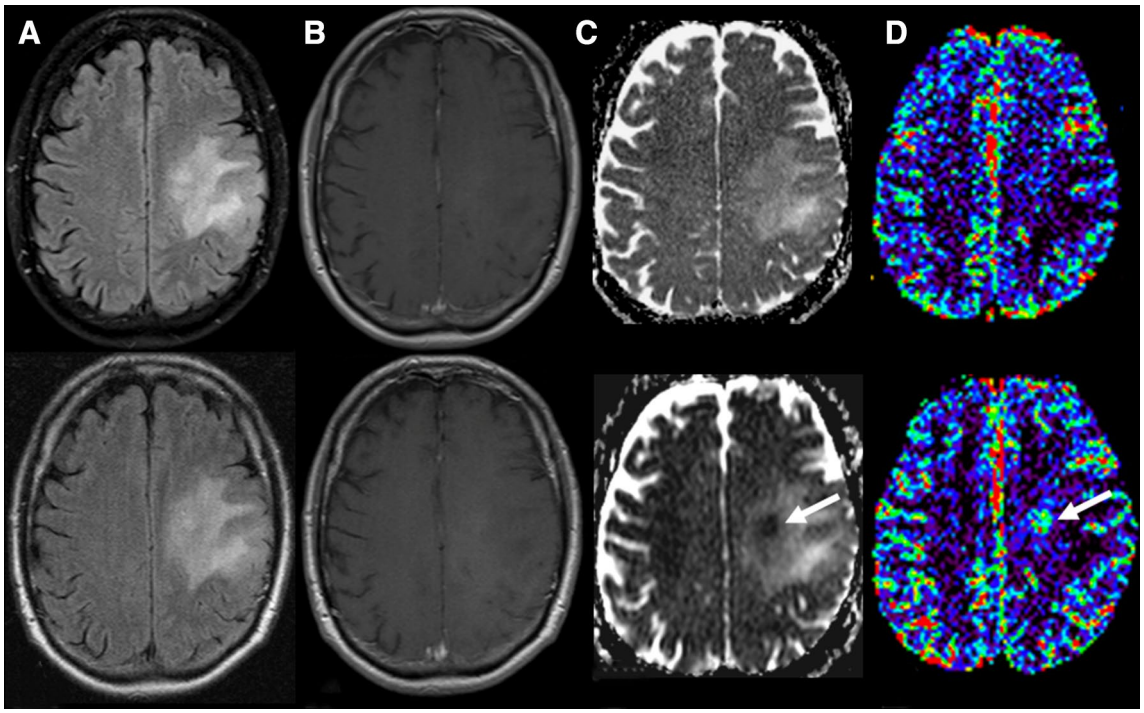

Fig. 2 Initial (upper row) and follow-up MRI (lower row) examination after 4 months in a 53-year-old patient with glioblastoma with GC growth pattern. **a** FLAIR images demonstrate widespread hyperintensities in the left hemisphere. **b** Contrast-enhanced T1-weighted images demonstrate no contrast enhancement. **c** Initial ADC maps are unremarkable, whereas follow-up ADC maps show a focal area of reduced ADC (arrow). **d** Initial rCBV maps are unremarkable, whereas follow-up rCBV maps show a focal area of increased rCBV (arrow)

regional variations in rADC in non-enhancing regions of glioblastoma have been reported earlier and demonstrated to be associated with more aggressive histopathologic tumor features [9, 10]. Furthermore, the occurrence of focal areas with restricted diffusion during treatment and consecutive development of enhancing tumor in these areas have been reported previously in patients with glioblastoma [21]. Admittedly, in another study on GC, the authors reported an increased or normal rADC in the majority of patients, whereas a decreased rADC was found only in one case with presence of a focal mass [14]. However, in this study no differentiation between WHO grade II, III, and IV was undertaken, and no further comparison to localized glioblastoma was performed.

On PWI, glioblastoma with GC growth pattern showed a similar rCBV compared to the surrounding T2 lesion in localized glioblastoma. This stands in contrast to earlier studies which reported a decreased to normal rCBV in GC [14, 22, 23]. These discrepancies might easily be explained by the fact that no differentiation between WHO grade II, III, and IV was undertaken in these studies. The described focal areas with increased rCBV in glioblastoma with disseminated growth patterns most likely reflect the localized microvascular alterations within the tumor. Similar regional variations in rCBV in contrast-enhancing regions of glioblastoma have been reported in the past [9, 10] and were demonstrated to be associated with more aggressive histopathologic tumor features. Recently it has been demonstrated that rCBV provides a reliable estimation of microvessel density in high grade glioma [24], reflecting the abnormal angiogenesis with numerically increased, aberrant calibred, and tortuous vessels.

Consequently, thorough evaluation of DWI and PWI may reveal focal areas of reduced rADC and/or increased rCBV in an otherwise uniformly appearing tumor and thus might be helpful to detect areas with increased cellular density and/or abnormal tumor vessels. On the long run, this may result in a more precise description and grading of a brain tumor with GC growth pattern. Besides this, a more precise description of glioblastoma with GC growth pattern by use of DWI and PWI, will facilitate the planning of stereotactic or open biopsy and consequently could increase the accuracy of histopathological diagnosis as already reported for glioma in general [12]. Furthermore, details of DWI and PWI might also be useful for target volume definition in adjuvant radiotherapy these patients will need to undergo, as recently suggested for patients with recurrent high-grade gliomas [25].

The present study has several limitations. First, this is a retrospective study with limited sample size. However, to our knowledge this is the first study focusing on a detailed

evaluation of rADC and rCBV in glioblastoma with GC growth pattern. Second, due to the study design, a control group with patients has been compiled retrospectively. Although we matched control subjects to the patients in the GC group according to age, gender, and IDH mutation, we cannot completely exclude a selection bias. Third, there is a large variability of reported rADC (ranging from 1.054 to 2.01) [26–29] and rCBV values (ranging from 1.05 to 3.21) [26–31] in the peritumoral T2 lesion in glioblastoma in the available medical literature. However, the determined rADC and rCBV values in the present study are in the range of earlier study results, and the inclusion of a control group with localized glioblastoma should facilitate the interpretation of the data as well as improve the comparability with previous studies. Finally, the study was performed with different MRI scanners and different imaging sequences. However, the MRI sequences have been customized for optimal comparability in daily clinical routine and consequently should be generally comparable.

In conclusion, lower rADC in glioblastoma with GC growth pattern might reflect the diffuse tumor cell infiltration whereas the focal areas with decreased rADC and/or increased rCBV probably indicate high tumor cell density and/or abnormal tumor vessels which may be useful for biopsy guidance and radiotherapy target volume definition and dosing.

Compliance with ethical standards

Conflict of interest Alex Förster: none. Stefanie Brehmer received travel support from Carl Zeiss Meditec AG. Marcel Seiz-Rosenhagen: none. Iris Mildenberger: none. Frank A. Giordano serves as consultant and speaker for Carl Zeiss Meditec AG, NOXXON Pharma AG, Merck Serono GmbH, Roche Pharma AG, Siemens Healthcare Diagnostics GmbH, and holds patents related with Carl Zeiss Meditec AG. Holger Wenz: none. David Reuss: none. Daniel Hänggi: none. Christoph Groden: none.

Ethical approval This study has been approved by the local institutional review board (Medizinische Ethikkommission II der Medizinischen Fakultät Mannheim) and has therefore been performed in accordance with the ethical standards laid down in the 1964 Declaration of Helsinki and its later amendments. Patient consent was waived for this analysis by the local institutional review board due to its retrospective nature.

References

1. Stupp R, Mason WP, van den Bent MJ, Weller M, Fisher B, Taphoorn MJ, Belanger K, Brandes AA, Marosi C, Bogdahn U, Curschmann J, Janzer RC, Ludwin SK, Gorlia T, Allgeier A, Lacombe D, Cairncross JG, Eisenhauer E, Mirimanoff RO (2005) Radiotherapy plus concomitant and adjuvant temozolomide for glioblastoma. N Engl J Med 352(10):987–996
2. Stupp R, Hegi ME, Mason WP, van den Bent MJ, Taphoorn MJ, Janzer RC, Ludwin SK, Allgeier A, Fisher B, Belanger K, Hau P, Brandes AA, Gijtenbeek J, Marosi C, Vecht CJ, Mokhtari K, Wesseling P, Villa S, Eisenhauer E, Gorlia T, Weller M, Lacombe D, Cairncross JG, Mirimanoff RO (2009) Effects of radiotherapy with concomitant and adjuvant temozolomide versus radiotherapy alone on survival in glioblastoma in a randomised phase III study: 5-year analysis of the EORTC-NCIC trial. Lancet Oncol 10(5):459–466
3. Scherer J (1940) The forms of growth in gliomas and their practical significance. Brain 40:631–635
4. Holland EC (2000) Glioblastoma multiforme: the terminator. Proc Natl Acad Sci USA 97(12):6242–6244
5. Thomas RP, Xu LW, Lober RM, Li G, Nagpal S (2013) The incidence and significance of multiple lesions in glioblastoma. J Neurooncol 112(1):91–97
6. Wesseling P, Capper D (2018) WHO 2016 classification of gliomas. Neuropathol Appl Neurobiol 44(2):139–150
7. Carpio-O'Donovan R, Korah I, Salazar A, Melancon D (1996) Gliomatosis cerebri. Radiology 198(3):831–835
8. Chen S, Tanaka S, Giannini C, Morris J, Yan ES, Buckner J, Lachance DH, Parney IF (2013) Gliomatosis cerebri: clinical characteristics, management, and outcomes. J Neurooncol 112(2):267–275
9. Barajas RF Jr, Hodgson JG, Chang JS, Vandenberg SR, Yeh RF, Parsa AT, McDermott MW, Berger MS, Dillon WP, Cha S (2010) Glioblastoma multiforme regional genetic and cellular expression patterns: influence on anatomic and physiologic MR imaging. Radiology 254(2):564–576
10. Barajas RF Jr, Phillips JJ, Parvataneni R, Molinaro A, Essock-Burns E, Bourne G, Parsa AT, Aghi MK, McDermott MW, Berger MS, Cha S, Chang SM, Nelson SJ (2012) Regional variation in histopathologic features of tumor specimens from treatment-naive glioblastoma correlates with anatomic and physiologic MR Imaging. Neuro Oncology 14(7):942–954
11. Peretti-Viton P, Brunel H, Chinot O, Daniel C, Barrie M, Bouvier C, Figarella-Branger D, Fuentes S, Dufour H, Grisoli F (2002) Histological and MR correlations in Gliomatosis cerebri. J Neurooncol 59(3):249–259
12. Gempt J, Soehngen E, Forster S, Ryang YM, Schlegel J, Zimmer C, Meyer B, Ringel F, Grams AE, Forschler A (2014) Multimodal imaging in cerebral gliomas and its neuropathological correlation. Eur J Radiol 83(5):829–834
13. Yu A, Li K, Li H (2006) Value of diagnosis and differential diagnosis of MRI and MR spectroscopy in gliomatosis cerebri. Eur J Radiol 59(2):216–221
14. Desclee P, Rommel D, Hernalsteen D, Godfraind C, de Coene B, Cosnard G (2010) Gliomatosis cerebri, imaging findings of 12 cases. J Neuroradiol 37(3):148–158
15. Constans JM, Collet S, Kauffmann F, Hossu G, Dou W, Ruan S, Rioult F, Derlon JM, Lechapt-Zalcmann E, Chapon F, Valable S, Theron J, Guillamo JS, Courtheoux P (2011) Five-year longitudinal MRI follow-up and (1)H single voxel MRS in 14 patients with gliomatosis treated with temodal, radiotherapy and antiangiogenic therapy. Neuroradiol J 24(3):401–414
16. Boxerman JL, Schmainda KM, Weisskoff RM (2006) Relative cerebral blood volume maps corrected for contrast agent extravasation significantly correlate with glioma tumor grade, whereas uncorrected maps do not. AJNR Am J Neuroradiol 27(4):859–867
17. Tatu L, Moulin T, Bogousslavsky J, Duvernoy H (1996) Arterial territories of human brain: brainstem and cerebellum. Neurology 47(5):1125–1135
18. Tatu L, Moulin T, Bogousslavsky J, Duvernoy H (1998) Arterial territories of the human brain: cerebral hemispheres. Neurology 50(6):1699–1708
19. Rorden C, Karnath HO, Bonilha L (2007) Improving lesion-symptom mapping. J Cogn Neurosci 19(7):1081–1088

20. Stummer W (2007) Mechanisms of tumor-related brain edema. Neurosurg Focus 22(5):E8
21. Gupta A, Young RJ, Karimi S, Sood S, Zhang Z, Mo Q, Gutin PH, Holodny AI, Lassman AB (2011) Isolated diffusion restriction precedes the development of enhancing tumor in a subset of patients with glioblastoma. AJNR Am J Neuroradiol 32(7):1301–1306
22. Yang S, Wetzel S, Law M, Zagzag D, Cha S (2002) Dynamic contrast-enhanced T2*-weighted MR imaging of gliomatosis cerebri. AJNR Am J Neuroradiol 23(3):350–355
23. Rizzo L, Crasto SG, Moruno PG, Cassoni P, Ruda R, Boccaletti R, Brosio M, De Lucchi R, Fava C (2009) Role of diffusion- and perfusion-weighted MR imaging for brain tumour characterisation. Radiol Med 114(4):645–659
24. Hu LS, Eschbacher JM, Dueck AC, Heiserman JE, Liu S, Karis JP, Smith KA, Shapiro WR, Pinnaduwage DS, Coons SW, Nakaji P, Debbins J, Feuerstein BG, Baxter LC (2012) Correlations between perfusion MR imaging cerebral blood volume, microvessel quantification, and clinical outcome using stereotactic analysis in recurrent high-grade glioma. AJNR Am J Neuroradiol 33(1):69–76
25. Wang B, Zhao P, Zhang Y, Ge M, Lan C, Li C, Pang Q, Xu S, Liu Y (2018) Quantitative dynamic susceptibility contrast perfusion-weighted imaging-guided customized gamma knife re-irradiation of recurrent high-grade gliomas. J Neurooncol 139(1):185–193
26. Chiang IC, Kuo YT, Lu CY, Yeung KW, Lin WC, Sheu FO, Liu GC (2004) Distinction between high-grade gliomas and solitary metastases using peritumoral 3-T magnetic resonance spectroscopy, diffusion, and perfusion imagings. Neuroradiology 46(8):619–627
27. Rollin N, Guyotat J, Streichenberger N, Honnorat J, Tran VM, Cotton F (2006) Clinical relevance of diffusion and perfusion magnetic resonance imaging in assessing intra-axial brain tumors. Neuroradiology 48(3):150–159
28. Tsougos I, Svolos P, Kousi E, Fountas K, Theodorou K, Fezoulidis I, Kapsalaki E (2012) Differentiation of glioblastoma multiforme from metastatic brain tumor using proton magnetic resonance spectroscopy, diffusion and perfusion metrics at 3 T. Cancer Imaging 12:423–436
29. Neska-Matuszewska M, Bladowska J, Sasiadek M, Zimny A (2018) Differentiation of glioblastoma multiforme, metastases and primary central nervous system lymphomas using multiparametric perfusion and diffusion MR imaging of a tumor core and a peritumoral zone-searching for a practical approach. PLoS ONE 13(1):e0191341
30. Law M, Cha S, Knopp EA, Johnson G, Arnett J, Litt AW (2002) High-grade gliomas and solitary metastases: differentiation by using perfusion and proton spectroscopic MR imaging. Radiology 222(3):715–721
31. Lehmann P, Saliou G, de Marco G, Monet P, Souraya SE, Bruniau A, Vallee JN, Ducreux D (2012) Cerebral peritumoral oedema study: does a single dynamic MR sequence assessing perfusion and permeability can help to differentiate glioblastoma from metastasis? Eur J Radiol 81(3):522–527

Affiliations

Alex Förster[1] · Stefanie Brehmer[2] · Marcel Seiz-Rosenhagen[2] · Iris Mildenberger[3] · Frank A. Giordano[4] · Holger Wenz[1] · David Reuss[5,6] · Daniel Hänggi[2] · Christoph Groden[1]

[1] Department of Neuroradiology, University Medical Center Mannheim, Medical Faculty Mannheim, University of Heidelberg, Theodor-Kutzer-Ufer 1-3, 68167 Mannheim, Germany

[2] Department of Neurosurgery, University Medical Center Mannheim, Medical Faculty Mannheim, University of Heidelberg, Mannheim, Germany

[3] Department of Neurology, University Medical Center Mannheim, Medical Faculty Mannheim, University of Heidelberg, Mannheim, Germany

[4] Department of Radiation Oncology, University Medical Center Mannheim, Medical Faculty Mannheim, University of Heidelberg, Mannheim, Germany

[5] Department of Neuropathology, University Hospital Heidelberg, Heidelberg, Germany

[6] Clinical Cooperation Unit Neuropathology, German Cancer Consortium (DKTK), German Cancer Research Center (DKFZ), Heidelberg, Germany